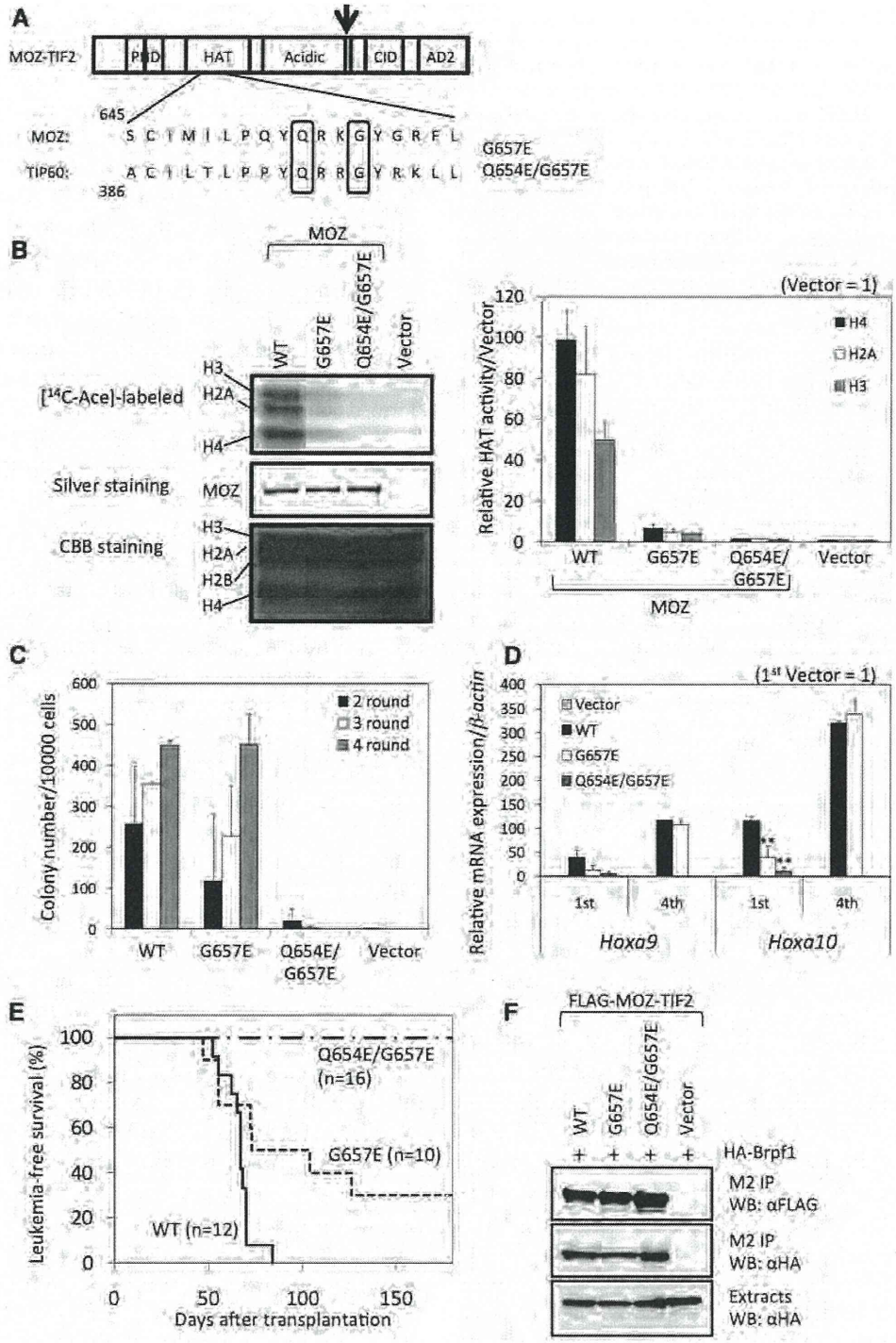

The antibodies used in these experiments are the same as written above for MOZ and Brpf1, and anti-acetyl-Histone H3 (Upstate), and anti-Histone H3 (abcam).

Statistical analysis

Statistical significance was determined by two-tailed Student *t* test.

Results

Brpf1 is required for immortalization of MOZ–TIF2 leukemic cells

Previous studies have suggested that BRPF1 forms complex with MOZ, and interacts directly to MOZ at N-terminal

◀ **Fig. 3** HAT activity of MOZ is required for transformation activity by MOZ–TIF2. **a** Structure of MOZ–TIF2 and its point mutants, Q654E/G657E and G654E. **b** HAT activity of WT and point mutants of MOZ. WT, G654E, Q654E/G657E MOZ or empty vector were cotransfected into 293FT cells. Immunoprecipitates were collected and cultured with histone H2A/B, H3, H4 and C^{14} labeled-acetyl-coenzyme A. C^{14} labeled acetylated histone was detected by BAS. Although HAT activity was reduced in both point mutants of MOZ compared to WT MOZ, G657E MOZ retained subtle HAT activity. Data are mean ± SD ($n = 3$). **c** Colony numbers of cells transduced with WT, G654E, Q654E/G657E MOZ–TIF2 or empty vector. WT and G657E MOZ–TIF2 showed transformation activity, which was not observed in cells transduced with Q654E/G657E MOZ–TIF2 or empty vector. **d** First round and 4th round colonies of cells transduced with WT, G654E, Q654E/G657E MOZ–TIF2 or empty vector were collected and analyzed for expression levels of *Hoxa9, Hoxa10* by qRT-PCR analysis. Expression level of *Hoxa10* was significantly lower in colony cells transduced with both mutants compared to WT MOZ–TIF2 at 1st round, but reached to the similar levels at 4th round in cells with Q654E/G657E MOZ–TIF2. Data are mean ± SD ($n = 3$). $^{**}P < .01$. **e** Kaplan–Meier survival curve analysis of mice transplanted with WT, G657E or Q654E/G657E MOZ–TIF2. All of the mice transplanted with WT MOZ–TIF2 and 7 out of 10 mice transplanted with G657E MOZ–TIF2 developed AML, while none of the mice transplanted with Q654E/G657E MOZ–TIF2 developed leukemia. **f** FLAG-tagged WT, G654E, Q654E/G657E MOZ–TIF2 or empty vector were cotransfected into 293FT cells together with HA-tagged Brpf1. Immunoprecipitates with anti-FLAG antibody (M2 IP) or cell lysates (Extracts) were subjected to immunoblotting with anti-HA or anti-FLAG antibodies. WT and both point mutants of MOZ–TIF2 were able to interact with Brpf1

domain [18]. Thus, we firstly constructed deletion mutant of BRPF1 (Δ1–222) which lacks interacting domain with MOZ, and performed immunoprecipitation assay. This mutant BRPF1 consistently lacked potential to form complex with MOZ (Fig. 1a). Using wild-type (WT) and deletion mutant of BRPF1, we next examined the effect of *Brpf1* knockdown in MOZ–TIF2 leukemic cells. MOZ–TIF2-tranduced mouse BM cells were subsequently transduced with Brpf1 shRNA by lentivirus system. Knockdown efficiencies were confirmed by qRT-PCR and western blotting (Fig. 1b, c). *Brpf1* knockdown resulted in marked decrease of colony numbers, which was rescued by WT human BRPF1 but not by mutant human BRPF1 (Fig. 1d). We further examined the effect of *Brpf1* knockdown on transcriptional activation induced by MOZ–TIF2. As expected, *Brpf1* knockdown led to decrease of *Hoxa9*, *Hoxa10* and *Meis1* expression (Fig. 1E). This decrease was again restored by WT human BRPF1 but not by mutant human BRPF1. These data suggest that Brpf1 contributes to *Hoxa9, Hoxa10* and *Meis1* transcription, which are overexpressed in AML patients with MOZ fusions [15].

Interacting domain of MOZ with Brpf1 is essential for initiation of MOZ–TIF2 leukemia

To investigate the importance of MOZ interaction with Brpf1, we firstly constructed several MOZ–TIF2 mutants as shown in Fig. 2a, and performed immunoprecipitation assay. The 760–783 region of MOZ was previously reported to be the interacting domain with BRPF1 [18]. However, deletion of the region 760–783 did not affect interaction of MOZ–TIF2 with BRPF1 in our condition (Fig. 2b). We previously found that the 760–783 region is required for histone acetyltransferase (HAT) activity [1]. Deletion analysis showed that there is another interacting domain that localized at HAT domain (N488–664) (Fig. 2c). For the following assay, we selected two deletion mutants of MOZ–TIF2, previously reported mutant Δ760–783, and Δ311–664 which lacks the novel interacting domain. We transduced these two deletion mutants, WT MOZ–TIF2 or empty vector to BM progenitors and performed colony formation assay. While WT MOZ–TIF2 cells were capable of forming colonies for several times of replating, others including two deletion mutants of MOZ–TIF2 lost their ability to form colonies in the 2nd round (Fig. 2d). 1st round colony cells were collected and analyzed for expression levels of *Hoxa9*, *Hoxa10* and *Meis1* by qRT-PCR. Corresponding to the results of colony formation assay, transcriptional activation of *Hoxa9* and *Hoxa10* induced by WT MOZ–TIF2 was not observed by two deletion mutants (Fig. 2f). Furthermore, none of the mice injected with BM cells transduced with either of the deletion mutants of MOZ–TIF2 developed AML (Fig. 2e).

HAT activity of MOZ contributes to leukemic transformation induced by MOZ–TIF2

The 760–783 and 488–664 regions were localized in MOZ HAT domain [1]. Although HAT activity is reported to be dispensable for leukemogenesis by MOZ–TIF2 [10], we evaluated the possible association between lack of MOZ HAT activity and loss of leukemogenic potential in Δ311–664 or Δ760–783 mutant MOZ–TIF2. MOZ is the founding member of the MYST family of HATs, which share the conserved MYST domains [5]. To assess the importance of MOZ HAT activity, we constructed previously reported MOZ HAT-deficient G657E mutant as well as Q654E/G657E mutant according to the HAT-deficient mutant of TIP60 (Fig. 3a) [8, 19, 20]. Firstly, we assessed HAT activity of these two HAT-deficient mutants using immunoprecipitates with anti-FLAG antibody, obtained from 293FT cells transfected with FLAG-tagged WT or mutant MOZ (Fig. 3b). WT MOZ showed HAT activity for Histones H2A, H3, H4. Although both HAT-deficient mutants G657E and Q654E/G657E possessed markedly low HAT activity compared to WT MOZ, HAT activity slightly remained in G657E mutant. Next, we examined the colony formation activity of these two HAT-deficient mutants. BM progenitors were transduced with WT, G657E, Q654E/G657E mutant of MOZ–TIF2 or empty vector and subsequently cultured in methylcellulose media. Through 4 rounds of replating, WT and G657E mutant, but not Q654E/G657E mutant, were capable of

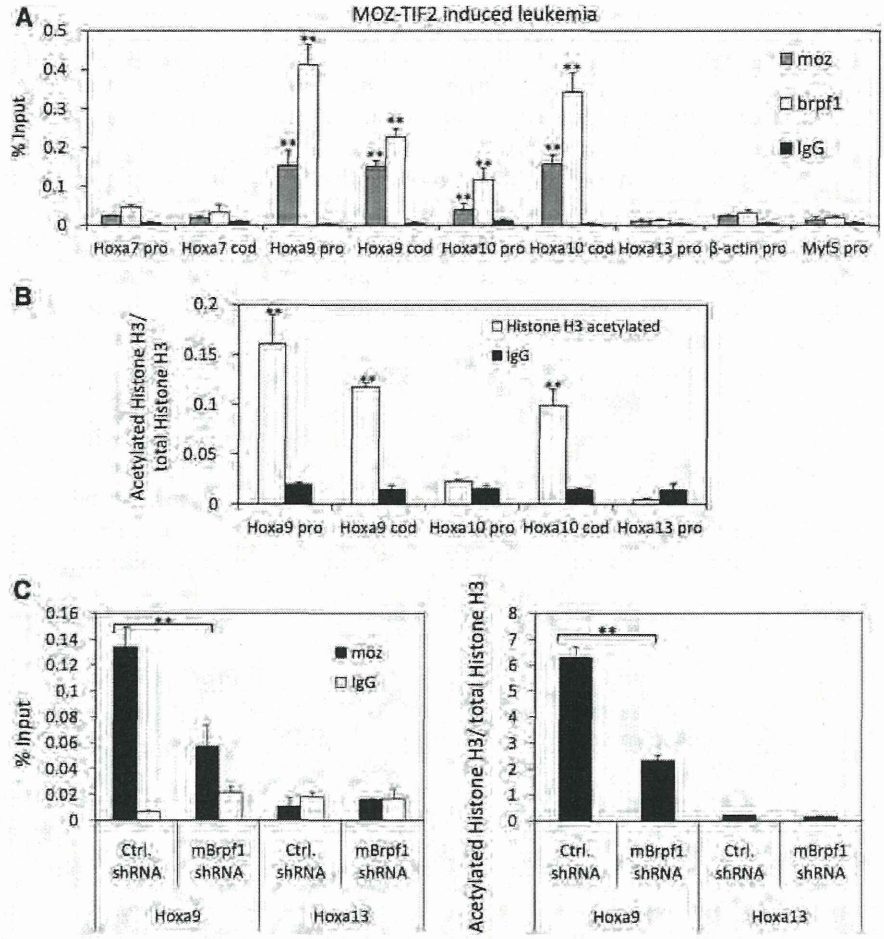

Fig. 4 *Hoxa9* and *Hoxa10* are direct targets of Moz and Brpf1. **a, b** Relative binding of Moz, Brpf1 and acetylated Histone H3 to the promoter and coding region of indicated genes in MOZ–TIF2 leukemic cells. Moz and Brpf1 colocalized at *Hoxa9* and *Hoxa10* genes, in which acetylated Histone H3 levels were higher compared to other tested genes. Data are mean ± SD ($n = 3$). $^{**}P < .01$. **c** Relative binding of Moz and acetylated Histone H3 to the promoter region of *Hoxa9* and *Hoxa13* after *Brpf1* knockdown. Downregulation of Brpf1 reduced the localization of Moz on promoter region of Hoxa9 and also reduced Histone H3 acetylation. Data are mean ± SD ($n = 3$). $^{**}P < .01$

inducing serial replating activity (Fig. 3c). *Hoxa10* expression levels of the 1st round colony cells were decreased by both mutants, but increased to similar level as WT in the 4th round by G657E mutant (Fig. 3d). BM progenitors transduced with WT, G657E or Q654E/G657E mutant of MOZ–TIF2 were also transplanted into sublethally irradiated recipient mice. G657E mutant MOZ–TIF2 led to development of AML in a subset of mice as reported before [8]. However, Q654E/G657E mutant MOZ–TIF2 showed no potential to initiate leukemia (Fig. 3e). These two HAT-deficient mutants were confirmed to be capable of interacting with Brpf1 at similar level as WT MOZ–TIF2 (Fig. 3f). These results indicate that even in a slight level, MOZ HAT activity is required for leukemogenic activity induced by MOZ–TIF2, which was independent of interaction with Brpf1.

Hoxa9 and *Hoxa10* are direct targets of MOZ and BRPF1 complex

To understand the mechanism of leukemic transformation induced by MOZ–TIF2, we performed chromatin immunoprecipitation (ChIP) assay using MOZ–TIF2 colony cells. As shown in Fig. 4a, MOZ and Brpf1 colocalized on chromatin within *Hoxa9* and *Hoxa10* locus, suggesting that these genes are direct targets of MOZ and Brpf1 complex. Indeed, Histone H3 acetylation level was upregulated at target *Hoxa9* and *Hoxa10* genes (Fig. 4b). We also performed ChIP assay using Brpf1 shRNA expressing MOZ–TIF2 colony cells. Depletion of Brpf1 resulted in reduction of MOZ localization on target *Hoxa9* gene, suggesting that Brpf1 enhances the enrichment level of MOZ localization on target genes (Fig. 4c). Together, these data suggest that Brpf1 leads to MOZ localization on the target genes, *Hoxa9* and *Hoxa10*, which enhance histone H3 acetylation and transcriptional activation of these genes, eventually resulting in development of AML.

Hoxa9 overexpression is not substantial for transformation of MOZ–TIF2 in Brpf1 downregulated cells

Previously, HOXA9 alone was reported to be sufficient for leukemic transformation in vitro [11, 13]. Because MOZ–

TIF2 leukemic cells exhibited lower expression level of *Hoxa9,* we assessed the effect of HOXA9 overexpression in MOZ–TIF2 leukemic cells with *Brpf1* knockdown. Unexpectedly, enforced expression of human HOXA9 failed to restore colony formation ability that was impaired by *Brpf1* knockdown (Fig. 5a, b). Downregulation of endogenous *Hoxa9, Hoxa10* and *Meis1* by depletion of Brpf1 was not restored by HOXA9 overexpression (Fig. 5c), suggesting again that Brpf1 contributes to transcriptional activation of not only *Hoxa9* but also *Hoxa10* and *Meis1*, both of which do influence the leukemic transformation activity. [12, 14, 21, 22].

Discussion

HOX genes are deregulated in a subset of AML patients, which strongly correlate with poor prognosis [23, 24]. Human AML with MOZ fusions applies to this subset of group, with high levels of *HOXA9* and *HOXA10* [15]. Herein, upregulation of *HOX* genes may contribute to the leukemogenesis in MOZ-related AML. To assess the mechanism and the role of *HOX* genes deregulation in MOZ-related leukemias, we focused on Brpf1. Brpf1, a component of MOZ complex, possesses PHD finger domain, bromodomain and PWWP domain [16, 17, 25]. PWWP domain and bromodomain of Brpf1 directly bind to Histones and are required for chromatin targeting by Brpf1 [16]. Previous study in zebrafish and medaka suggested that Brpf1 is required for the maintenance of *Hox* genes expression through Moz-dependent histone acetylation. [16, 17] Thus, Brpf1 may contribute to upregulation of *HOX* genes in MOZ-related leukemias.

In this study, we have demonstrated that Brpf1 plays an important role in leukemogenesis induced by MOZ–TIF2. Our data indicated that *Hoxa9* and *Hoxa10* were direct

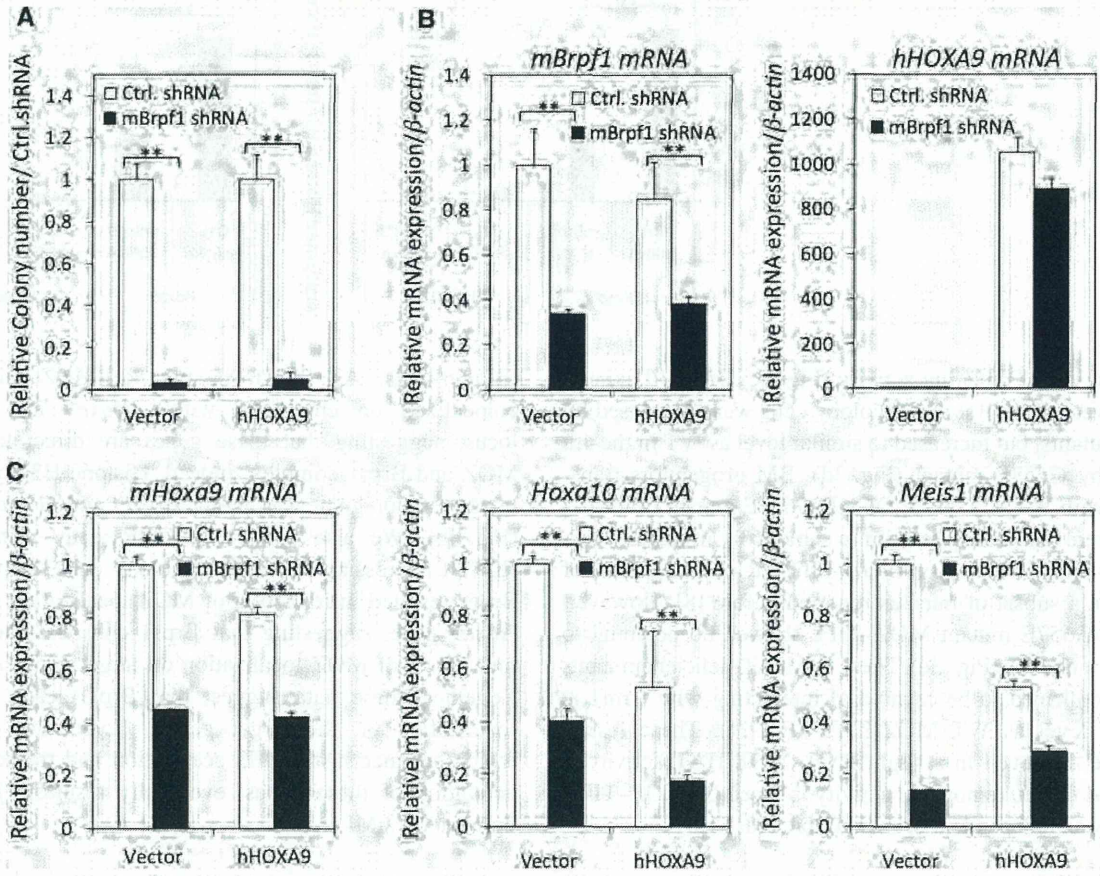

Fig. 5 Effect of HOXA9 overexpression on MOZ–TIF2 leukemic cells with downregulated Brpf1. **a** Relative colony number of MOZ–TIF2 leukemic cells transduced with control shRNA or Brpf1 shRNA. Overexpression of wild-type HOXA9 was not sufficient to restore colony formation activity of MOZ–TIF2 leukemic cells with downregulated Brpf1. Data are mean ± SD ($n = 3$). $^{**}P < .01$. **b** Expression of murine *Brpf1* and human *HOXA9* after Brpf1 shRNA and HOXA9 overexpression. **c** Effects of Brpf1 shRNA and HOXA9 overexpression on expression levels of *Hoxa9, Hoxa10* and *Meis1* in Brpf1 downregulated MOZ–TIF2 leukemic cells. Reduced expressions of *Hoxa9, Hoxa10* and *Meis1* by *Brpf1* knockdown were sustained in cells with HOXA9 overexpression. Data are mean ± SD ($n = 3$). $^{**}P < .01$

targets of MOZ and BRPF1 in MOZ–TIF2 leukemic cells. Because depletion of Brpf1 exhibited decreased level of MOZ localization on these target genes, resulting in loss of transformation ability induced by MOZ–TIF2, we suggest that Brpf1 promotes MOZ to localize on chromatin of these target genes. Brpf1 recruits MOZ to the target genes and upregulates transcriptional activation through histone H3 acetylation. Since binding of MOZ–TIF2 to the *Meis1* gene locus is weak compared to its binding to *Hoxa9* and *Hoxa10* (data not shown), MOZ–TIF2 is unlikely to regulate the expression of Meis1 directly. Our data also indicate that HAT activity of MOZ is essential for transformation activity induced by MOZ–TIF2. HAT-deficient MOZ–TIF2 was incapable of not only deregulating *Hox* genes, but also initiating leukemia. We suggest that MOZ or MOZ-fusion/BRPF1 complex upregulates *HOX* genes mediated by MOZ-dependent histone acetylation, which finally leads to the development of leukemia.

Although HOXA9 alone possesses transformation activity, enforced expression of human HOXA9 unexpectedly failed to rescue transformation activity abolished by Brpf1 depletion. There are two possible reasons to be considered. Firstly, *Hoxa10* and *Meis1*, both of which were downregulated in Brpf1 depleted cells remained in lower level compared to control cells despite HOXA9 overexpression. This may suggest that downregulation of several *HOX* genes other than *HOXA9* may result in loss of leukemic transformation. Secondly, Brpf1 may be required for HOXA9 function and its downstream pathway. Further study is required to determine the association of Brpf1 and Hoxa9 in the maintenance of transformation activity in AML cells.

Previously, we have shown that upregulation of M-CSFR is critical for the regulation of AML stem cells in MOZ–TIF2 leukemia, and STAT5, which was highly phosphorylated in M-CSFR high cells but not in low cells, may contribute to the clonal expansion and stem cell maintenance [2]. In this study, we demonstrated that deletion mutant of MOZ–TIF2 lacking interacting domain with Brpf1 lost its transformation activity. However, M-CSFR upregulation was maintained in BM cells transduced with this mutant MOZ–TIF2. Furthermore, Hoxa9 expression was upregulated in both M-CSFR-high cells and low cells [2]. Therefore, MOZ/BRPF1/HOX pathway should be considered as independent of PU.1/M-CSFR pathway (Fig. 6). Collectively, our study reveals that MOZ/BRPF1/HOX pathway plays a crucial role in the development of leukemia induced by MOZ–TIF2. For efficient induction of AML, block in the normal hematopoietic differentiation program together with unrestrained growth is required. Several AML-associated chromosomal translocations require additional mutations for the progenitors to gain both of these functions [26, 27]. However, in terms of MOZ–TIF2 leukemia, although increased expression of *HOX* genes may be insufficient to induce AML in a short period, increased phosphorylation of STAT5 mediated by PU.1/M-CSFR pathway would accelerate the development of leukemia. Thus, both MOZ/BRPF1/HOX pathway and PU.1/M-CSFR pathway are essential for the development of MOZ–TIF2 AML.

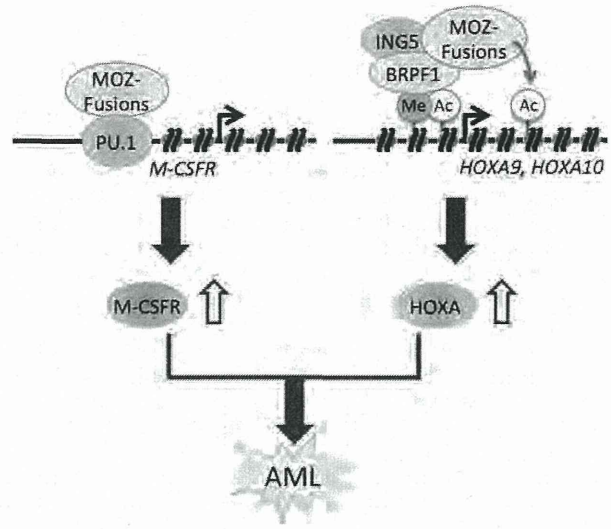

Fig. 6 Model of leukemogenic mechanism induced by MOZ–TIF2. Apart from PU.1/M-CSFR pathway, BRPF1/HOX pathway is essential for leukemogenesis by MOZ–TIF2. BRPF1 enhances the localization of MOZ on target genes such as *HOXA9* or *HOXA10*, and promotes Histone H3 acetylation, which may result in transcriptional upregulation of target genes, finally contributing to the development of leukemia

Acknowledgments This work was supported in part by Grants-in-Aid from the Ministry of Health, Labor, and Welfare; the Ministry of Education, Culture, Sports, Science, and Technology; and National Cancer Center Research and Development Fund.

Conflict of interest The authors declare no competing financial interests.

References

1. Kitabayashi I, Aikawa Y, Nguyen LA, et al. Activation of AML1-mediated transcription by MOZ and inhibition by the MOZ–CBP fusion protein. EMBO J. 2001;20(24):7184–96.
2. Aikawa Y, Katsumoto T, Zhang P, et al. PU.1-mediated upregulation of CSF1R is crucial for leukemia stem cell potential induced by MOZ–TIF2. Nat Med. 2010;16(5):580–5.
3. Rokudai S, Aikawa Y, Tagata Y, et al. Monocytic leukemia zinc finger (MOZ) interacts with p53 to induce p21 expression and cell-cycle arrest. J Biol Chem. 2009;284(1):237–44.
4. Katsumoto T, Aikawa Y, Iwama A, et al. MOZ is essential for maintenance of hematopoietic stem cells. Genes Dev. 2006;20(10):1321–30.
5. Borrow J, Stanton VP Jr, Andresen JM, et al. The translocation t(8;16)(p11;p13) of acute myeloid leukaemia fuses a putative

acetyltransferase to the CREB-binding protein. Nat Genet. 1996;14:33–41.
6. Kitabayashi I, Aikawa Y, Yokoyama A, et al. Fusion of MOZ and p300 histone acetyltransferases in acute monocytic leukemia with a t(8;22)(p11;q13) chromosome translocation. Leukemia. 2001;15:89–94.
7. Chaffanet M, Gressin L, Preudhomme C, et al. MOZ is fused to p300 in an acute monocytic leukemia with t(8;22). Genes Chromosomes Cancer. 2000;28:138–44.
8. Deguchi K, Ayton PM, Carapeti M, et al. MOZ–TIF2-induced acute myeloid leukemia requires the MOZ nucleosome binding motif and TIF2-mediated recruitment of CBP. Cancer Cell. 2003;3:259–71.
9. Yang XJ, Ullah M. MOZ and MORF, two large MYSTic HATs in normal and cancer stem cells. Oncogene. 2007;26:5408–19.
10. Carapeti M, Aguiar RC, Goldman JM, et al. A novel fusion between MOZ and the nuclear receptor coactivator TIF2 in acute myeloid leukemia. Blood. 1998;91:3127–33.
11. Calvo KR, Sykes DB, Pasillas M, Kamps MP. Hoxa9 immortalizes a granulocyte macrophage colony stimulating factor dependent promyelocyte capable of biphenotypic differentiation to neutrophils or macrophages independent of enforced Meis expression. Mol Cell Biol. 2000;20:3274–85.
12. Buske C, Feuring-Buske M, Antonchuk J, et al. Overexpression of HOXA10 perturbs human lymphomyelopoiesis in vitro and in vivo. Blood. 2001;97:2286–92.
13. Thorsteinsdottir U, Mamo A, Kroon E, et al. Overexpression of the myeloid leukemia associated Hoxa9 gene in bone marrow cells induces stem cell expansion. Blood. 2002;99:121–9.
14. Thorsteinsdottir U, Sauvageau G, Hough MR, et al. Overexpression of HOXA10 in murine hematopoietic cells perturbs both myeloid and lymphoid differentiation and leads to acute myeloid leukemia. Mol Cell Biol. 1997;17:495–505.
15. Camós M, Esteve J, Jares P, et al. Gene expression profiling of acute myeloid leukemia with translocation t(8;16)(p11;p13) and MYST3-CREBBP rearrangement reveals a distinctive signature with a specific pattern of HOX gene expression. Cancer Res. 2006;66(14):6947–54.
16. Hibiya K, Katsumoto T, Kondo T, et al. Brpf1, a subunit of the MOZ histone acetyl transferase complex, maintains expression of anterior and posterior Hox genes for proper patterning of craniofacial and caudal skeletons. Dev Biol. 2009;329(2):176–90.
17. Laue K, Daujat S, Crump JG, et al. The multidomain protein Brpf1 binds histones and is required for Hox gene expression and segmental identity. Development. 2008;135:1935–46.
18. Ullah M, Pelletier N, Xiao L, et al. Molecular architecture of quartet MOZ/MORF histone acetyltransferase complexes. Mol Cell Biol. 2008;28(22):6828–43.
19. Ikura T, Ogryzko VV, Grigoriev M, et al. Involvement of the TIP60 histone acetylase complex in DNA repair and apoptosis. Cell. 2000;102(4):463–73.
20. Perez-Campo FM, Borrow J, Kouskoff V, Lacaud G. The histone acetyl transferase activity of monocytic leukemia zinc finger is critical for the proliferation of hematopoietic precursors. Blood. 2009;113(20):4866–74.
21. Thorsteinsdottir U, Kroon E, Jerome L, et al. Defining roles of Hox and MEIS1 genes in induction of acute myeloid leukemia. Mol Cell Biol. 2001;21(1):224–34.
22. Kroon E, Krosl J, Thorsteinsdottir U, et al. Hoxa9 transforms primary bone marrow cells through specific collaboration with Meis1a but not Pbx1b. EMBO J. 1998;17(13):3714–25.
23. Golub TR, Slonim DK, Tamayo P, et al. Molecular classification of cancer: class discovery and class prediction by gene expression monitoring. Science. 1999;286:531–7.
24. Andreeff M, Ruvolo V, Gadgil S, et al. HOX expression patterns identify a common signature for favorable AML. Leukemia. 2008;22(11):2041–7.
25. Vezzoli A, Bonadies N, Allen MD, et al. Molecular basis of histone H3K36me3 recognition by the PWWP domain of Brpf1. Nat Struct Mol Biol. 2010;17(5):617–9.
26. Naoe T, Kiyoi H. Gene mutations of acute myeloid leukemia in the genome era. Int J Hematol. 2013;97(2):165–74.
27. Shima Y, Kitabayashi I. Deregulated transcription factors in leukemia. Int J Hematol. 2011;94(2):134–41.

Cancer Science
Japanese Cancer Association JCA
Open Access

Nuclear export signal within CALM is necessary for CALM-AF10-induced leukemia

Mai Suzuki,[1] Kazutsune Yamagata,[1] Mika Shino,[1] Yukiko Aikawa,[1] Koichi Akashi,[2] Toshio Watanabe[3] and Issay Kitabayashi[1]

[1]Division of Hematological Malignancy, National Cancer Center Research Institute, Tokyo; [2]Department of Medicine and Biosystemic Science, Kyushu University Graduate School of Medical Science, Fukuoka; [3]Department of Biological Science, Graduate School of Humanities and Sciences, Nara Women's University, Nara, Japan

Key words

AF10, chromosome translocation, histone modification, leukemia, nuclear export signal

Correspondence

Issay Kitabayashi, Division of Hematological Malignancy, National Cancer Center Research Institute, Tsukiji 5-1-1, Chuo-ku, Tokyo 104-0045, Japan.
Tel: +81-3-3542-2511; Fax: +81-3-3542-0688;
E-mail: ikitabay@ncc.go.jp

Funding Information

Ministry of Health, Labor, and Welfare. Ministry of Education, Culture, Sports, Science, and Technology. National Cancer Center Research and Development Fund. Naito Foundation. Cosmetology Research Foundation. Nara Women's University Intramural Grant for Project Research.

Received September 16, 2013; Revised December 5, 2013; Accepted December 30, 2013

Cancer Sci **105** (2014) 315–323

doi: 10.1111/cas.12347

The *CALM–AF10* fusion gene, which results from a t(10;11) translocation, is found in a variety of hematopoietic malignancies. Certain *HOXA* cluster genes and *MEIS1* genes are upregulated in patients and mouse models that express CALM-AF10. Wild-type clathrin assembly lymphoid myeloid leukemia protein (CALM) primarily localizes in a diffuse pattern within the cytoplasm, whereas AF10 localizes in the nucleus; however, it is not clear where CALM-AF10 acts to induce leukemia. To investigate the influence of localization on leukemogenesis involving CALM-AF10, we determined the nuclear export signal (NES) within CALM that is necessary and sufficient for cytoplasmic localization of CALM-AF10. Mutations in the NES eliminated the capacity of CALM-AF10 to immortalize murine bone-marrow cells *in vitro* and to promote development of acute myeloid leukemia in mouse models. Furthermore, a fusion of AF10 with the minimal NES can immortalize bone-marrow cells and induce leukemia in mice. These results suggest that during leukemogenesis, CALM-AF10 plays its critical roles in the cytoplasm.

The chromosome translocation t(10;11)(p13;q14), found in T-cell acute lymphoblastic leukemia (T-ALL), acute myeloid leukemia (AML) and malignant lymphomas, results in the fusion of the clathrin assembly lymphoid myeloid leukemia protein (*CALM*) and *AF10* [1,2]. The CALM–AF10 fusion protein consists of almost all CALM and AF10 proteins, with the exception of one or two plant homeodomain (PHD).[1,3] AF10, also known as MLLT10, interacts with the transcription factor Ikaros and H3K4me3 through its octapeptide motif–leucine zipper (OM-LZ) region and PHD domains, respectively.[4–6] In both mice and humans, CALM-AF10 upregulates certain *HOXA* cluster genes (*HOXA5*, *HOXA7*, *HOXA9* and *HOXA10*) and *MEIS1*.[7,8] *Hoxa5* upregulation, which is critical for CALM-AF10-induced leukemogenesis,[9,10] is mediated by an interaction between the AF10 OM-LZ region and the histone methyltransferase DOT1L, resulting in H3K79 hypermethylation at the *Hoxa5* locus.[9] These findings suggest that CALM-AF10 might function in the nucleus.

The CALM protein shuttles between the cytoplasm and the nucleus under the control of a CRM1-dependent nuclear export signal (NES).[11] In contrast to AF10, which localizes in the nucleus,[4] CALM-AF10 primarily localizes in the cytoplasm.[6,9] Other fusion partners of AF10 in acute myeloid and lymphoid leukemias include MLL, DDX3 and HNRNPH1.[12,13] MLL and hnRNPH1 primarily localize in the nucleus,[14,15] whereas DDX3, like CALM, is mostly distributed throughout the cytoplasm.[16,17] These observations prompted us to investigate whether CALM-AF10 exerts its function in the nucleus or the cytoplasm. We found that mutant CALM-AF10 lacking the NES localized in the nucleus and lost its ability to induce leukemia in mice. Conversely, a fusion consisting of the minimal NES and AF10 localized in the cytoplasm and induced leukemia. These results indicate that the cytoplasmic location of CALM-AF10 is critical for its role in leukemogenesis.

Materials and Methods

Generation of *CALM-AF10* mutant constructs. Plasmid encoding pcDNA3β-FLAG-CALM-AF10 was a gift from Y. Zhang (Department of Biochemistry and Biophysics, University of North Carolina).[9] Plasmid encoding the NES-deficient mutant FLAG-CALM^{NES4A}-AF10 and FLAG-CALM^{NES4A} were generated by introducing four point mutations into the CALM NES sequence by inverse PCR using a site-specific mutagenesis kit (Toyobo, Osaka, Japan).[18] Specifically, leucine (L)-544, L-547, L-551 and isoleucine (I)-553 in the putative NES sequence within CALM-AF10 were replaced by alanine (A), using the following primers: L544A, 5′-GCAGCCAACCTTGTGG

GCAATCTTGGC-3′, and 5′-AGATGAATCCAAGTCATCAGA TACT-3′; L547A, 5′-GCTGTGGGCAATCTTGGCATCGGAA AT-3′, and 5-′GTTGGCTGCAGATGAATCCAAGTCA-3′; L551A, 5′-GCTGGCATCGGAAATGGAACCACTAAG-3′, and 5′-ATT GCCCACAGCGTTGGCTGCAGAT-3′; I553A, 5′-GCCGGAAA TGGAACCACTAAGAATGAT-3′, and 5′-GCCAGCATTGCCC ACAGCGTTGGCT-3′. All mutations were confirmed by DNA sequencing. The AF10 sequence encoding amino acids 81–1027 (mAF10) was amplified by PCR and cloned into pcDNA3β-FLAG. To generate the fusion of the minimal NES with AF10, NES1 (amino acids 543–554) or NES2 (amino acids 539–558) within CALM was generated by PCR amplification using FLAG-CALM-AF10 as a template, and then cloned into pcDNA3β-FLAG-mAF10. The pMY-IG-FLAG-CALM-AF10-IRES-GFP, pMY-IG-FLAG-CALM^{NES4A}-AF10-IRES-GFP, pMY-IG-FLAG-mAF10-IRES-GFP and pMY-IG-FLAG-NES2-AF10-IRES-GFP constructs were generated by inserting the corresponding cDNA into the pMY-IG/IRES-GFP vector.

Cell culture and transfection. COS-7 cells were maintained in DMEM supplemented with 10% FBS, 100 U/mL penicillin, 100 μg/mL streptomycin and 2 mM L-glutamine at 37°C in a humidified 5% CO_2 incubator. COS-7 cells were transfected with pcDNA3β-FLAG constructs using the Effectene Transfection Reagent (Qiagen, Hilden, Germany).

Immunofluorescence analysis. Forty-eight hours after transfection, COS-7 cells transfected with pcDNA3β-FLAG constructs were fixed with 3.7% formaldehyde in PBS and examined by immunofluorescence staining with anti-FLAG M2 monoclonal antibody (Sigma-Aldrich, St. Louis, MO, USA), followed by secondary Alexa Fluor 488-conjugated goat anti-mouse IgG (Invitrogen, Carlsbad, CA, USA). Stained cells were mounted in VECTASHIELD mounting medium and observed using a BX50 fluorescence microscope (Olympus, Tokyo, Japan). Cytospins of murine bone-marrow cells transduced with pMY-IG/IRES-GFP viral constructs encoding FLAG-CALM-AF10, FLAG-CALM^{NES4A}-AF10, FLAG-NES2-AF10 or FLAG-mAF10 were fixed with 4% paraformaldehyde and stained with anti-FLAG M2 monoclonal antibody (Sigma-Aldrich) and anti-KMT4/DOT1L polyclonal rabbit antibody (Abcam, Cambridge, MA, USA), followed by secondary Alexa Fluor 568-conjugated goat anti-mouse IgG (Invitrogen) and Alexa Fluor 488-conjugated goat anti-rabbit IgG (Invitrogen), respectively. Stained bone-marrow cells were mounted in VECTASHIELD mounting medium with DAPI (Vector Laboratories, Burlingame, CA, USA) or Prolong Gold (Invitrogen) and observed under a BZ-9000 fluorescence microscope (Keyence Corporation, Osaka, Japan) or a FluoView FV10i confocal laser scanning microscopy (Olympus).

Retroviral infection and bone-marrow transplantation. C57BL/6J mice were purchased from CLEA Japan (Tokyo, Japan). All mouse experiments were approved by the National Cancer Center Animal Ethics Committee and performed in accordance with the institutional guidelines. The pMY-IG/IRES-GFP constructs encoding FLAG-CALM-AF10, FLAG-CALM^{NES4A}-AF10, FLAG-NES2-AF10 or FLAG-mAF10 were transfected into PLAT-E cells using the GeneJuice transfection reagent (Novagen, Nottingham, UK), and retrovirus supernatants were collected 48 h after transfection. c-kit$^+$ cells (1×10^5 cells), selected from murine total bone-marrow cells using CD117 MicroBeads (Miltenyi Biotec, Bergisch Gladbach, Germany), were incubated with the retrovirus and RetroNectin (Takara Bio, Madison, WI, USA) for 24 h in StemPro-34 SFM medium (Invitrogen) containing cytokines (20 ng/mL SCF, 10 ng/mL IL-6 and 10 ng/mL IL-3). The transduced donor bone-marrow cells were then transplanted into lethally irradiated (9.5 Gy) 7–8-week-old female C57BL/6J recipient mice by intravenous injection. For secondary transplants, bone-marrow cells from the primary leukemia mice were intravenously injected into sub-lethally irradiated (6 Gy) female C57BL/6J mice.

Serial-replating assay. Bone-marrow cells transduced with pMY-IG/IRES-GFP constructs encoding FLAG-CALM-AF10, FLAG-CALM^{NES4A}-AF10, FLAG-NES2-AF10 or FLAG-mAF10 were cultured for 3 days in methylcellulose medium (MethoCult M3234; StemCell Technologies, Vancouver, Canada) supplemented with murine SCF, IL-3 and GM-CSF. The GFP$^+$ cells in methylcellulose medium were then sorted using a JSAN cell sorter (Bay Bioscience, Kobe, Japan) and replated every 3–4 days in methylcellulose medium; colonies and cells were counted at each passage. Cells from the second-round and fifth-round colonies were harvested and analyzed by real-time PCR (RT-PCR).

Real time-PCR analysis. Total RNA from replating colonies was purified using an RNeasy Mini Kit (Qiagen). Purified RNA were reverse-transcribed into cDNA using the High Capacity cDNA Reverse Transcription Kit (Applied Biosystems, Foster City, CA, USA). Real-time PCR was performed using the 7500 Fast Real-time PCR System (Applied Biosystems) using the FastStart Universal Probe Master with ROX (Roche, Basel, Switzerland) and the following TaqMan probes (Applied Biosystems): *Hoxa5* (Mm04213381_s1), *Hoxa7* (Mm00657963_m1), *Hoxa9* (Mm00439364_m1), *Hoxa10* (Mm00433966_m1) and *Meis1* (Mm00487664_m1). The relative expression levels of these genes were normalized against the level of *Actb* (Mm00607939_s1).

Flow-cytometry analysis. Bone-marrow cells from leukemic mice were pre-incubated with rat IgG (Sigma-Aldrich), and then incubated on ice with the appropriate staining reagents: anti-CD115(CSF1R)-PE (eBioscience, San Diego, CA, USA), anti-Mac-1(M1/70)-PE-Cy7 (eBioscience), anti-Gr-1(RB6-8C5)-APC (BD Pharmingen, San Diego, CA, USA) and anti-c-Kit(2B8)-APC-eF780 (eBioscience). FACS analysis and cell sorting were performed using the JSAN cell sorter and the results were analyzed using the FLOWJO software (Tree Star, Standford, CA, USA).

Results

The nuclear export signal within CALM is required for cytoplasmic localization of CALM-AF10. To investigate the role of subcellular localization of CALM-AF10 in leukemogenesis, we focused on the NES within the CALM portion of the fusion protein (amino acids 543–554 of CALM).[9] We generated NES-deficient mutants CALM^{NES4A}-AF10 and CALM^{NES4A}, in which leucine-544, leucine-547, leucine-551 and isoleucine-553 in the putative NES region within CALM were substituted with alanines (NES4A) (Fig. 1a). Expression vectors for FLAG-tagged CALM-AF10, CALM, CALM^{NES4A}-AF10, CALM^{NES4A} and mAF10 (the AF10 portion of CALM-AF10) were transiently transfected into COS-7 cells. Immunofluorescence analysis revealed that CALM and CALM-AF10 primarily localized in the cytoplasm, whereas mAF10 and the NES mutants CALM^{NES4A}-AF10 and CALM^{NES4A} localized in the nucleus (Fig. 1b,c).

To determine the minimal NES, two sequences, NES1 (aa. 543–554) and NES2 (aa. 539–558), were fused to AF10 (Fig. 1a,b). As with mAF10, NES1-AF10 was in the nucleus; by contrast, NES2-AF10 was in the cytoplasm (Fig. 1d). The same results were obtained when these fusion proteins were transduced into murine hematopoietic progenitor cells by retro-

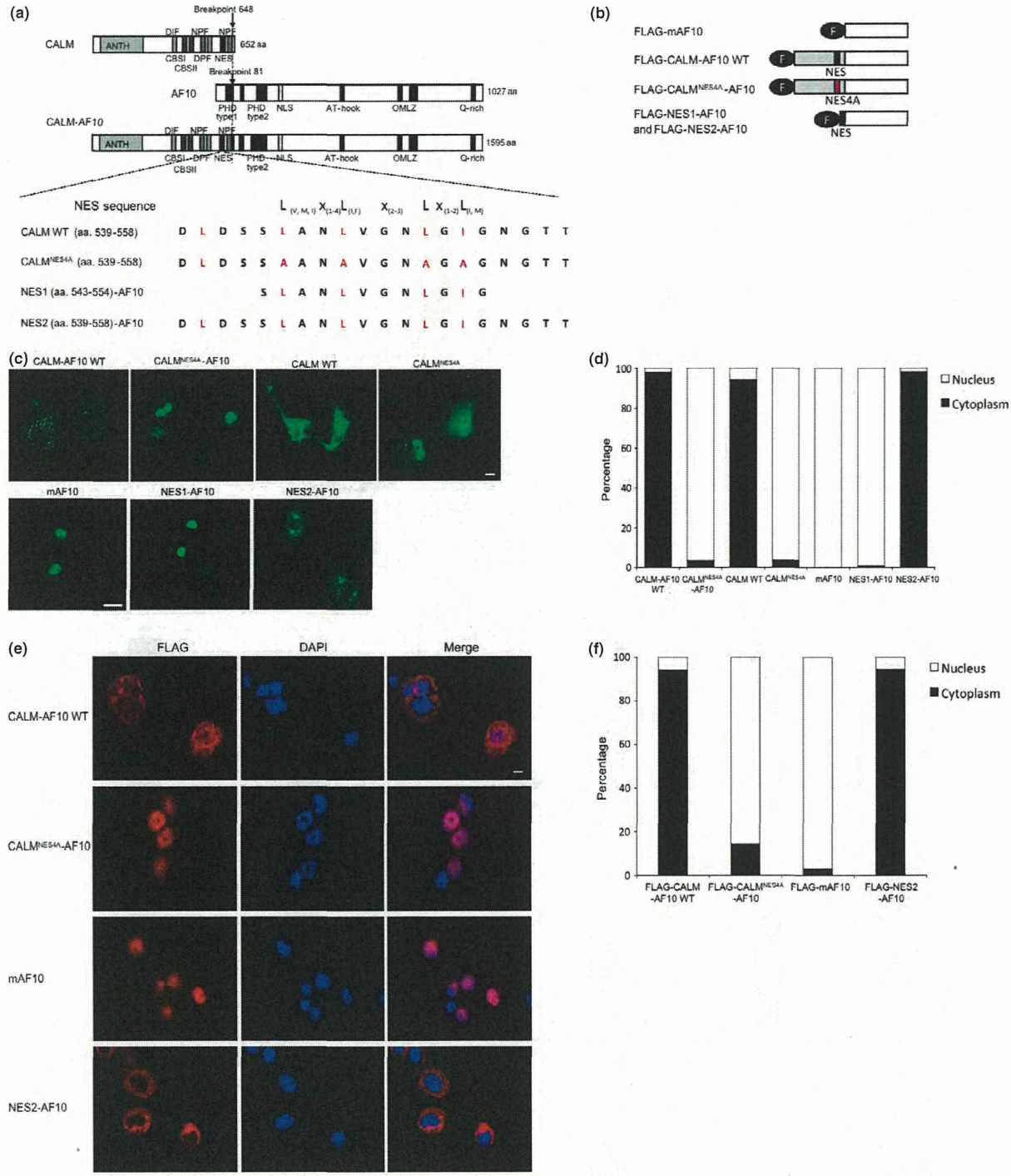

Fig. 1. The NES region within clathrin assembly lymphoid myeloid leukemia protein (CALM) is necessary for cytoplasmic localization. (a) Schematic representations of CALM, AF10, CALM-AF10 and mutant proteins. FLAG-CALM^{NES4A}-AF10 and FLAG-CALM^{NES4A} were generated by alanine substitution of three leucine residues and one isoleucine residue in the putative CALM NES (red). FLAG-NES1-AF10 and FLAG-NES2-AF10 mutants were constructed by fusion of the NES sequences of CALM to the AF10 portion of CALM-AF10. (b) Diagrams of the plasmid constructs used in transfection experiments. (c) Subcellular distribution of CALM-AF10 and the NES point mutations FLAG-CALM-AF10, FLAG-CALM, FLAG-CALM^{NES4A}-AF10, FLAG-CALM^{NES4A}, and FLAG-NES1-AF10, FLAG-NES2-AF10 and FLAG-mAF10 in COS-7 cells. Transfected cells were stained with anti-FLAG antibody (green) and observed by fluorescence microscopy. (d) Population of cells expressing transduced genes in the nucleus and cytoplasm shown in (c). (e) Subcellular distribution of CALM-AF10 and NES mutation proteins in murine bone-marrow cells. Transduced cells were stained with anti-FLAG antibody (red). (f) Population of cells expressing transduced genes in the nucleus and the cytoplasm shown in (e). Nuclei were stained with DAPI (blue) and observed by fluorescence microscopy. The scale bar represents 20 μm in (c) and 10 μm in (e). ANTH, AP180 N-terminal homology domain binding phosphatidylinositol 4,5-bisphosphate (PIP_2); DIF and DPF, motifs interacts with AP-2; NPF, a motif interacts with the EH (Eps15 homology) domain; CBS-I and -II, putative type I and II clathrin-binding sequences; NES, nuclear export signal; PHD Type1 and 2, plant homeodomain zinc finger domains; NLS, nuclear localization signal; AT-hook, DNA-binding protein motif; OMLZ, octapeptide motif-leucine zipper domain; Q-rich, glutamine-rich region.

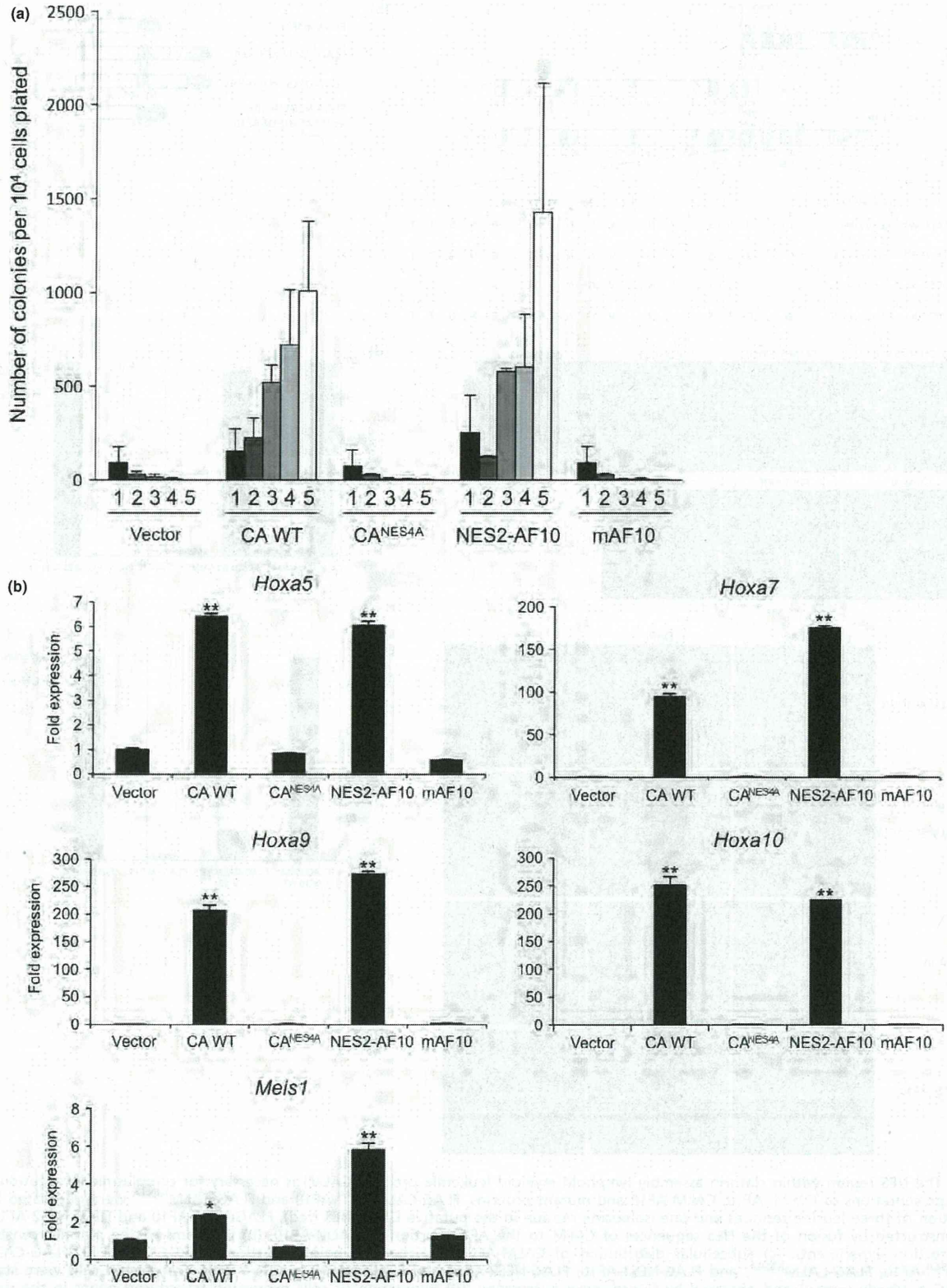

Fig. 2. The nuclear export signal within clathrin assembly lymphoid myeloid leukemia protein (CALM) is critical for *in vitro* immortalization of cells by CALM-AF10. (a) Serial colony-replating assays of murine bone-marrow cells transduced with FLAG-tagged wild-type and mutant CALM-AF10. In each round of replating, 3×10^4 transduced bone-marrow cells were plated. Bars represent the numbers of colonies. (b) *Hoxa* cluster and *Meis1* expression in cells transduced with wild-type or mutant CALM-AF10. RNA transcripts were analyzed by real-time PCR of murine bone-marrow cells transduced with wild-type and mutant CALM-AF10 *in vitro*. Expression levels of *Hoxa5*, *Hoxa7*, *Hoxa9*, *Hoxa10* and *Meis1* were normalized against *Actb* expression and compared with the levels in vector-transfected whole bone-marrow cells. Data are shown as means ± SEM from three independent samples. $^*P < 0.05$; $^{**}P < 0.01$. (*vs* normal bone-marrow cells). CA WT, wild-type CALM-AF10.